

Supporting Information

On-Resin Diels- Alder Reaction with Inverse Electron Demand: Efficient Ligation Method for Complex Peptides with Varying Spacer to Optimize Cell Adhesion

Mareen Pagel,^a René Meier,^a Klaus Braun,^b Manfred Wiessler,^b and Annette G. Beck-Sickinger^a

^aInstitute of Biochemistry, Faculty of Biosciences, Pharmacy and Psychology, Leipzig University, Leipzig, Germany; ^bDeutsches Krebsforschungszentrum, Im Neuenheimer Feld 280, 69120 Heidelberg, Germany

Table of contents

Supplementary Methods

Stability of Tetrazines on resin and in solution.....S2

Supplementary Results

Peptide Analytics.....S2

Absorption Measurement of Tetrazine Modified Resin.....S4

Stability of Tetrazines in Aqueous Environment on Resin and in Solution.....S4

Low Conversion of 1b with the Dienophiles 4,5 and 6.....S5

Protecting Groups Allyl and Alloc as Dienophiles in the DAR_{inv}.....S6

Instability of the DAR_{inv}- Product 8b During the CuAAC on Resin.....S7

Cell Adhesion on Negative Controls (8A, 8B, 8D) Containing c[**RADfK**(dienophile)]
Instead of c[**RGDfK**(dienophile)].....S8

MD-Simulation-Structure of Linkers.....S9

Supplementary References.....S10

Supplementary Methods

Stability of Tetrazines on Resin and in Solution

To assess the stability of tetrazines **2a** and **2b**, resin beads (**7a**, **7b**) were transferred into a 96-well plate and covered with 100 μ L H₂O per well at room temperature. The tetrazine absorption at 540 nm was measured every day and plotted normalized. Detailed information of the stability was gained by a cleavage of the peptides from the resin at 0 d and after 7 d by RP-HPLC and MALDI-ToF-MS analysis.

Stability in solution was tested with the purified peptides **1a** and **1b**. The peptides were dissolved in H₂O/tBuOH/ACN (3/1/0.1). The tetrazine absorption was measured at the absorption maximum of the compounds, which was slightly different than on resin (**2a** at 520 nm and **2b** at 530 nm) and plotted normalized. After 7 d incubation at room temperature the peptides were analyzed by RP-HPLC and MALDI-ToF-MS.

Supplementary Results

Peptide Analytics

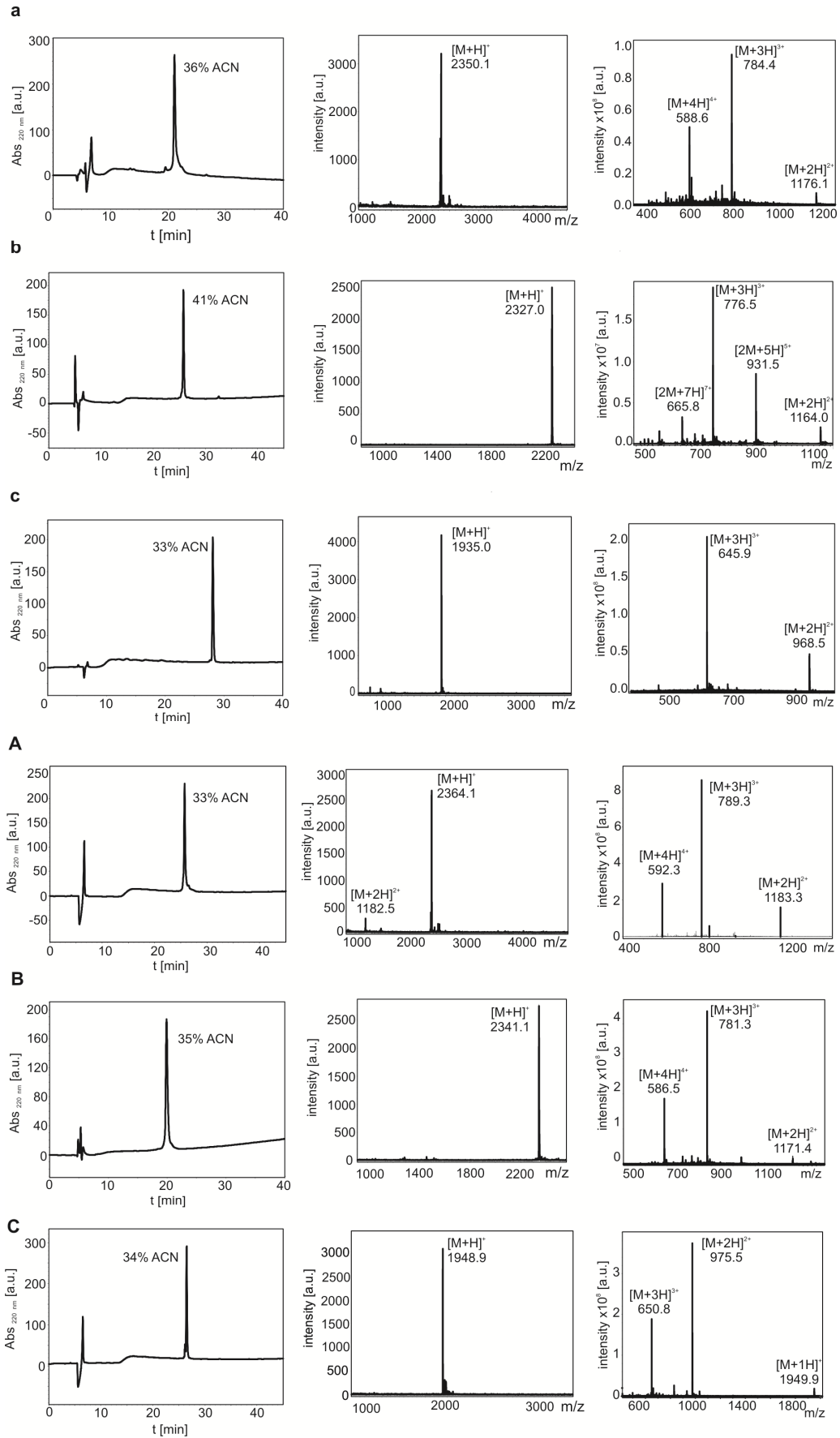
To evaluate the stability of tetrazines and to test cell adhesion on negative controls (RAD motif instead of RGD), following peptides were synthesized and analyzed as described.

Table S1 Peptide Analytics

entry	sequence	M [Da]	[M+H] ⁺	elution (%ACN) ^a	purity
1a	C-PEG-Y*-K(2a)-Y*-PEG-G*- β A-NH ₂	1461.7	1462.6	40	>90
1b	C-PEG-Y*-K(2b)-Y*-PEG-G*- β A-NH ₂	1440.6	1441.6	38	>80
8A	C-PEG-Y*-K((2a)(c[RADfK(Reppe)]))-Y*-PEG-G*- β A-NH ₂	2363.1	2364.1	33	>90
8B	C-PEG-Y*-K((2b)(c[RADfK(Reppe)]))-Y*-PEG-G*- β A-NH ₂	2340.2	2341.1	35 ^b	>90
8D	S-PEG-Y*-C(c[RADfK(maleimide)]))-Y*-PEG-G*- β A-NH ₂	1947.9	1948.9	34	>85

Peptides were analyzed by MALDI-ToF MS (Bruker, Daltonics) and RP-HPLC. The peptide purity was evaluated by two different HPLC systems using different columns and gradients; Gradients of eluent B (0.08 % TFA in ACN) in eluent A (0.1 % TFA in H₂O,) on a ^aPhenomenex Jupiter Proteo (90 Å, 5 μ m), ^bGrace Vydac C8 (300 Å, 5 μ m), Phenomenex Jupiter Proteo (300 Å, 4 μ m) and VariTide (200 Å, 6 μ m), PEG (polyethylene glycol), Y* (L-3,4-dihydroxyphenylalanine), G* (propargylglycine), β A (beta alanine)

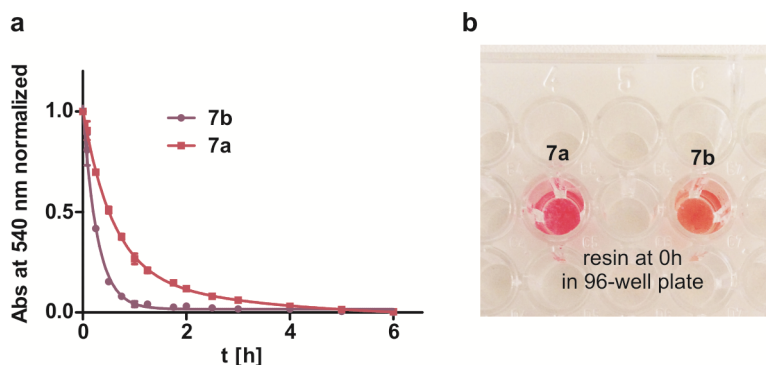
Tested Peptides were carefully analyzed by RP-HPLC and mass spectrometry. The obtained results are shown for **8a,b,d** and the negative controls **8A,B,D** in Supplementary Figure S1.



Supplementary Figure S1 RP-HPLC, MALDI-ToF-MS and ESI-ion-trap MS analysis of purified peptides (from left to right) ; analytics of a) 8a, b) 8b, c) 8d, A) 8A, B) 8B, C) 8D.

Absorption Measurement of Tetrazine Modified Resin

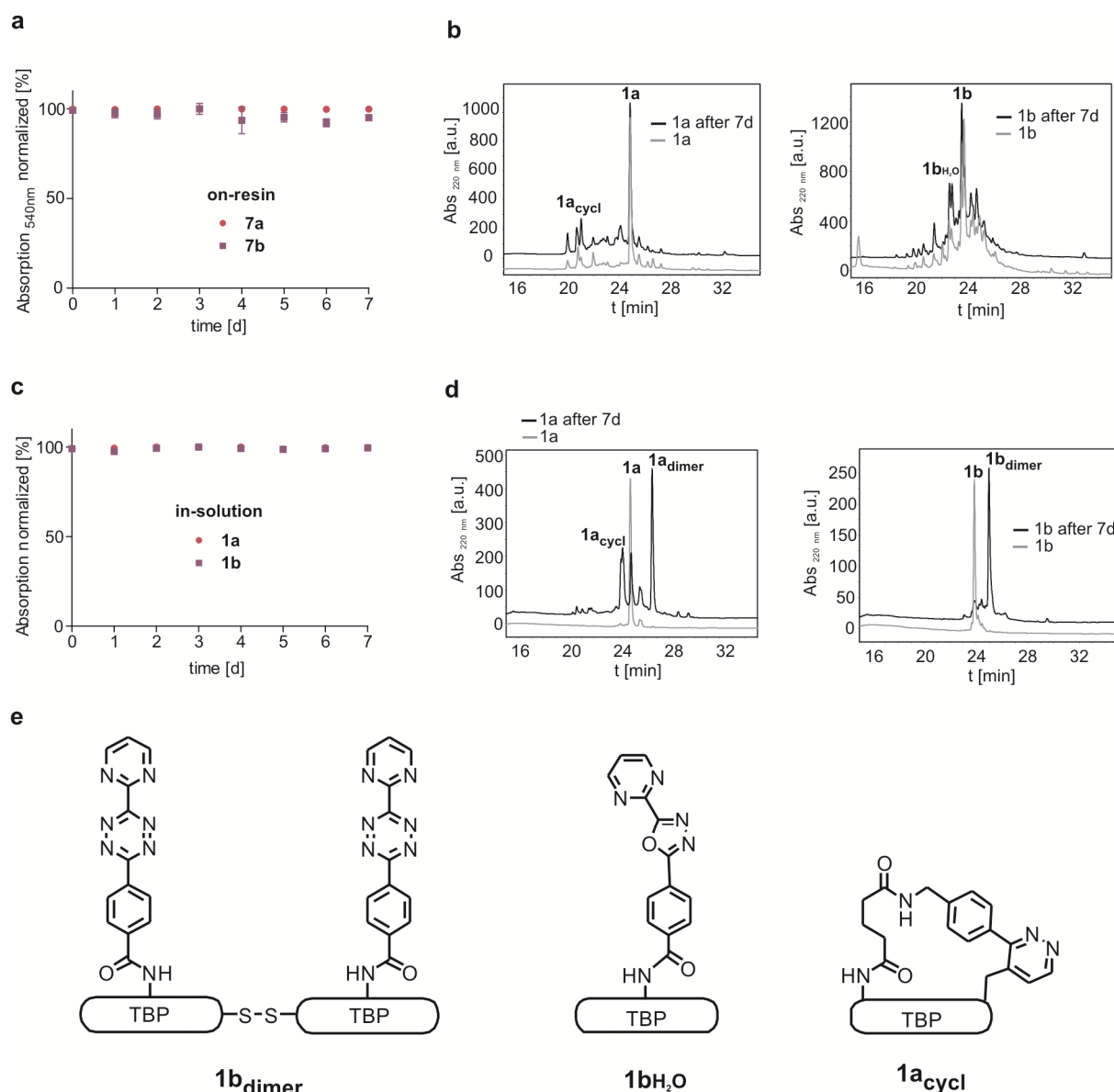
The DAR_{inv} can be easily monitored by direct measurement of the tetrazine absorption on resin by photometry with a multi plate reader in a 96-well plate (Supplementary Figure S2b). In Supplementary Figure S2a it is shown how the absorption maximum of the tetrazine decreases over time during the DAR_{inv} with peptide **3**. The experiment was repeated twice and showed very similar results.



Supplementary Figure S2 Absorption measurement of tetrazine on resin. a) Decrease of the normalized tetrazine absorption at 540 nm during the DAR_{inv} with resin bound peptides **7a** and **7b** (modified with tetrazines **2a** and **2b**) with dienophile **3**, $n=2$, mean \pm SEM. **b)** Experimental set-up to measure the tetrazine absorption on resin. Resin modified with **2a** and **2b** was transferred in a 96-well plate and incubated with the dissolved dienophile.

Stability of Tetrazines in Aqueous Environment on Resin and in Solution

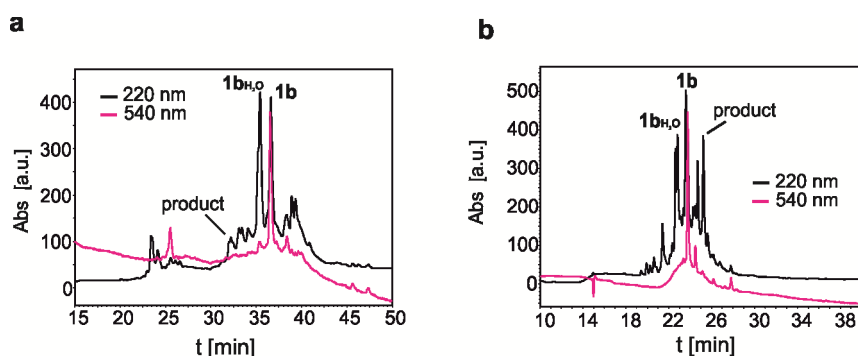
The stability of tetrazines was investigated as described in the supplementary methods. The absorption maximum of the tetrazines was stable over 7 d on resin and in solution (Supplementary Figure S3a,c). However, RP-HPLC and MALDI-ToF-MS analysis revealed more detailed information. On resin tetrazines are sufficiently stable and generate just a few side products. Peptide **1a** showed higher stability than **1b** on resin (Supplementary Figure S3b). Analysis of **1b** after 7 d incubation in H₂O revealed the formation of the fragment **1b**_{H₂O}. It should be noted that these fragments and side products were present already at the time point 0 (probably induced by cleavage from the resin and subsequent dissolving) and slightly increased after 7 d. Peptides **1a,b** in solution dimerized almost quantitatively because of the N-terminal Cys in the sequence of TBP (**1**) (Supplementary Figure S3d). In addition, **1a** formed after incubation for 7 d the cyclic peptide **1a**_{cyc} by the undesired DAR_{inv} between the tetrazine and the alkyne functionality of Pra.



Supplementary Figure S3 Stability of tetrazine on resin and in solution. **a)** Stability of the tetrazine specific absorption maximum over 7 d on resin suspended in H₂O, mean ± SEM. **b)** RP-HPLC of crude **1a** (right) and **1b** (left) before and after the incubation with H₂O for 7 d. **c)** Stability of tetrazine specific absorption maximum over 7 d in solution, mean ± SEM. **d)** RP-HPLC of purified **1a** (right) and **1b** (left) at 0 d and 7 d. **e)** Structures of hypothesized side products, fragments and dimers.

Low Conversion of **1b** with the Dienophiles **4,5** and **6**

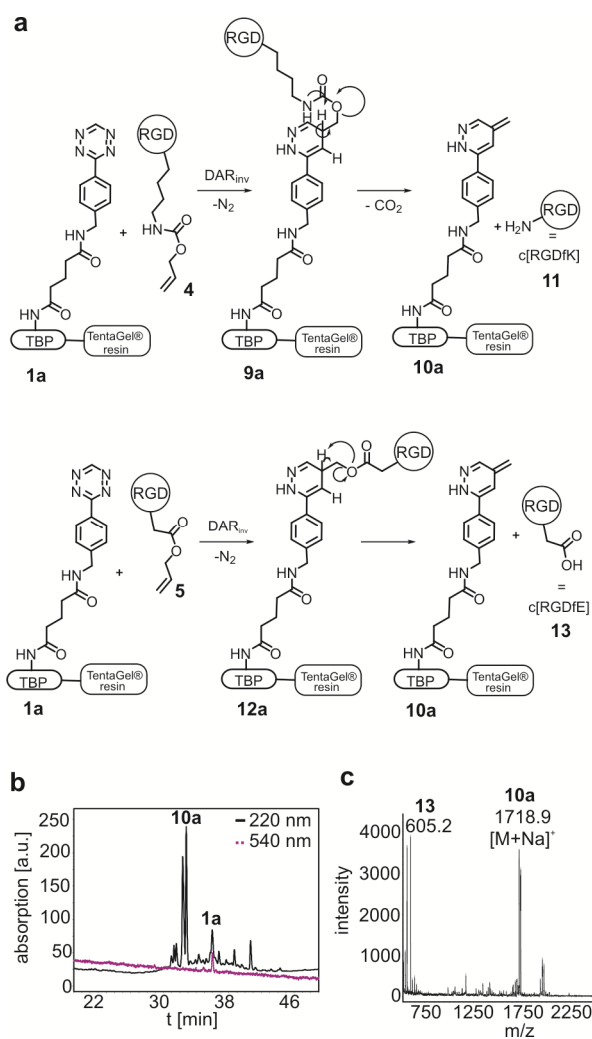
Cleavage of peptides from the resin and analysis by RP-HPLC and MALDI-ToF-MS after incubation with the dienophiles for 7 d showed that the desired products were formed. However, the fragment **1b_{H₂O}** and starting material were detected as well (see Supplementary Figure S4). Hence, it is stated that the reaction showed low conversion due to low stability and reactivity of tetrazine **2b**.



Supplementary Figure S4 Low conversion of tetrazine **1b with dienophile **4** and **6**.** **a)** RP-HPLC of the cleaved peptide mixture generated from the reaction of **1b** (Fmoc protected) and **4**. **b)** RP-HPLC of the cleaved peptide mixture generated from the reaction of **1b** and **6**.

Protecting Groups Allyl and Alloc as Dienophiles in the DAR_{inv}

To simplify the introduction of dienophiles into peptides we sought to test alkenes present in the amino- and carboxyl protecting groups alloc and ally. The cyclic peptides **4** and **5** were synthesized as described. After purification the dienophile bearing peptides were dissolved in $\text{H}_2\text{O}/\text{ACN}$ and incubated with **1a** bound on resin (Fmoc protected). Cleavage from the resin after 5 d incubation revealed no formation of the desired product. A m/z ratio of 1718.9 was found in the MALDI-ToF spectrum of both reactions (Supplementary Figure S5c). We hypothesize that the desired product is fragmented into **10a** releasing the unmodified c[RGDfK] (**11**) and c[RGDfE] (**13**) respectively (Supplementary Figure S5a). To test if the product degrades during acidic cleavage from the resin, **1a** was incubated with c[RGDfK(Alloc)] (**4**) in solution. However, a fragmentation was also detected in solution (not shown).

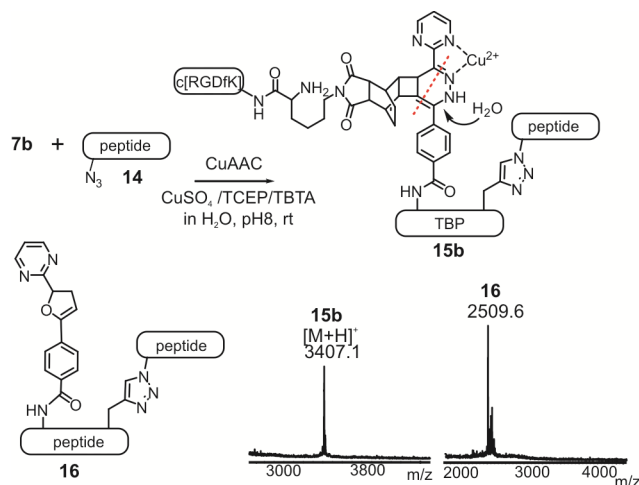


Supplementary Figure S5 a) DAR_{inv} of **1a** with $\text{c}[\text{RGDfK}(\text{Alloc})]$ (**4**) and $\text{c}[\text{RGDfE}(\text{Allyl})]$ (**5**) respectively and proposed fragmentation mechanism after cycloaddition. **b)** The Analysis by MALDI-ToF MS and **c)** RP-HPLC supports the formation of the shown fragment **10a** (Fmoc protected) and **13**.

Instability of the DAR_{inv} - Product **8b** during the CuAAC on Resin

For further modification of the peptide conjugate **8b**, a mixture of 2 eq $\text{CuSO}_4 \cdot 5 \text{H}_2\text{O}$ (0.01 M), 4 eq TCEP (0.1 M) and 0,2 eq $\text{tris}[(1\text{-benzyl-1H-1,2,3-triazol-4-yl)methyl}]\text{-amin}$ (TBTA) in H_2O (2 mM) was degassed with Ar and heated for 15 min at 37 °C. Then, 1 eq. of peptide **14** ($\text{K}(\text{N}_3)\text{FHRRIKA}$) was added to the mixture and the pH was adjusted to pH 8 with an aqueous NaOH solution ($c = 10 \text{ mM}$). Afterwards the resin was incubated with the reaction mixture, degassed with Ar and shaken for 24 h at rt. After filtration and washing, the resin was incubated for 2 h with an aqueous ethylenediaminetetraacetic acid (EDTA, 10 mM) solution to remove remained copper ions. Cleavage of the peptide from the resin revealed that the copper (I) catalyzed cycloaddition was in fact proceeding; however the resulting DAR_{inv} product **15b** was not stable under the conditions. Hence, a mixture of the product

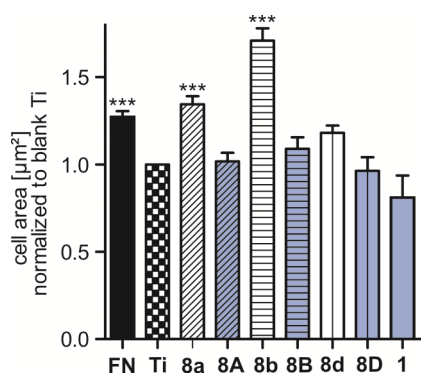
15b, the proposed fragment **16** and undefined side products was observed (Supplementary Figure S6). We propose a nucleophilic attack of H₂O with resulting N₂ release to yield **16**. A similar mechanism is shown for the hydrolysis of tetrazines.^{1,2} The fragmentation of **15b** may be enhanced by the presence of Cu ions that can be coordinated by the imino- and the pyridyl nitrogen as shown for tetrazines.³



Supplementary Figure S6 Combination of DAR_{inv} with CuAAC-Instability of 8b. Under the conditions of CuAAC on resin the desired product **15b** is not stable. The hypothesized mechanism is shown, yielding the fragment **16**, which could be identified by MALDI-ToF-MS of a RP-HPLC fraction. TCEP (Tris(2-carboxyethyl)phosphine), TBTA (Tris[(1-benzyl-1*H*-1,2,3-triazol-4-yl)methyl]amin)), rt (room temperature).

Cell Adhesion on Negative Controls (**8A**, **8B**, **8D**) Containing c[**RADfK**(dienophile)] Instead of c[**RGDfK**(dienophile)]

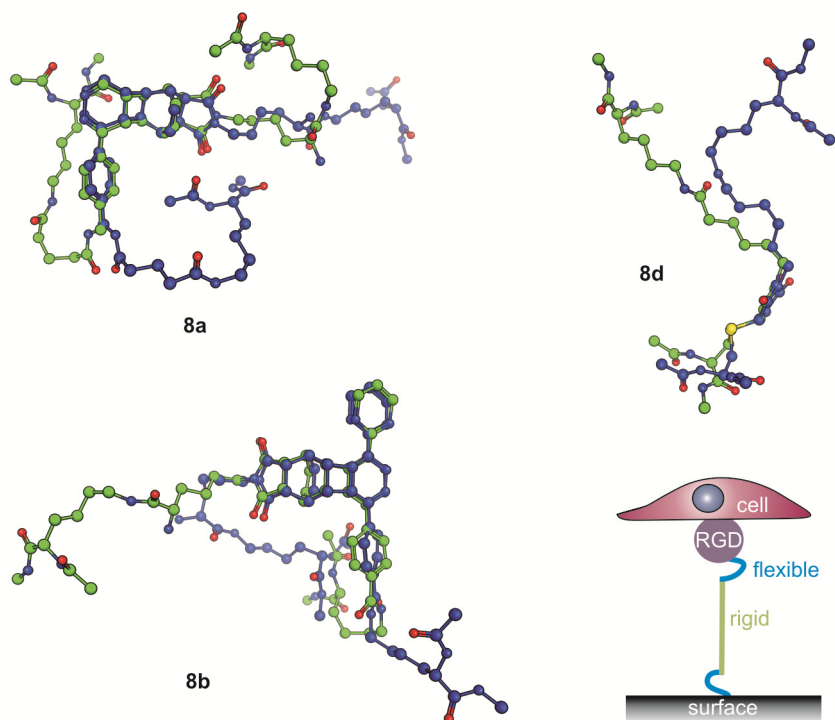
To check if the different linker moieties have a positive effect on cell adhesion, the negative controls **8A**, **8B** and **8D** were synthesized with a RGD to RAD exchange. Moreover, TBP (**1**) was tested for cell spreading. The surface anchor peptide TBP showed a smaller average cell size than cells grown on blank Ti, which is a result of the PEG chains in the peptide backbone, more detailed described in previous work by our group.⁴ The negative control c[**RADfK**] attached via different linkers to TBP showed no to very minor improvement of cell spreading compared to uncoated Ti (Supplementary Figure S7). This verifies that the improved cell response is mediated through the RGD-peptide and modulated by the structure of the linker as described.



Supplementary Figure S7 Cell adhesion on control peptides (blue). Average cell area after 6 h cell adhesion. Fibronectin (FN) coated Ti was used as positive and Ti (non coated titanium) as negative control. Data is presented as mean \pm SEM of $n \geq 3$, significant differences to blank Ti were determined by one-way ANOVA (** $p < 0.001$).

MD-Simulation-Structure of Linkers

Because of the high flexibility of the linker one most dominant conformation could not be identified. At room temperature the single bonds can rotate freely and many different conformations were adopted during the simulation. To identify the most frequent conformation for every linker we did a cluster analysis with a cluster criterion of 2 Å RMSD.⁵ All MD-Snapshots with a C α -C α distance bigger than 10 Å were clustered. Distances shorter than 10 Å were considered as artificial because of sterical hindrance in case of surface binding of the whole peptide. The two biggest clusters for each linker are shown in the Supplementary Figure S8. Due to the high flexibility of all linkers the two biggest clusters cover only a limited number of sampled conformations. **8a**: 5%, **8b**: 7%, **8d**: 13%. The interactions in the collapsed conformation are unspecific van-der-Waals interactions. We hypothesize that a suitable linker for RGD-mediated cell adhesion should consist of two short flexible ends that are connected by a long rigid structure (Supplementary Figure S8). Thereby, the RGD-peptide may be orientated freely by the flexible parts at the surface and close to the cell.



Supplementary Figure S8 Most occurring Structures of 8a,b,d. Depicted are the center structures of the biggest (blue atoms) and the second biggest (green atoms) cluster with Ca-Ca distances of: **8a**: 14.5Å and 11.6Å, **8b** 18.6Å and 10.8Å, **8d** 16.6Å and 16.2Å

Supplementary References

1. P. J. Snowdon, R. J. Whiteoak and J. D. Manley, *Fresenius J. Anal. Chem.*, 1991, **339**, 444-447.
2. R. Hoogenboom, B. C. Moore and U. S. Schubert, *J. Org. Chem.*, 2006, **71**, 4903-4909.
3. J. H. Cui, L. F. Huang, Z. Z. Lu, Y. Z. Li, Z. J. Guo and H. G. Zheng, *Crystengcomm*, 2012, **14**, 2258-2267.
4. M. Pagel, R. Hassert, T. John, K. Braun, M. Wiessler, B. Abel and A. G. Beck-Sickinger, *Angew. Chem. Int. Ed.*, 2016, **55**, 4826-4830.
5. X. Daura, K. Gademann, B. Jaun, D. Seebach, W. F. van Gunsteren and A. E. Mark, *Angew. Chem. Int. Ed.*, 1999, **38**, 236-240.